J. Biochem. **135**, 355–363 (2004)
DOI: 10.1093/jb/mvh043

Two Additional Carbohydrate-Binding Sites of β-Amylase from *Bacillus cereus* var. *mycoides* Are Involved in Hydrolysis and Raw Starch-Binding

Zhengmao Ye, Hideo Miyake*, Maki Tatsumi, Shigenori Nishimura and Yasunori Nitta†

Laboratory of Enzyme Chemistry, Graduate School of Agriculture and Biological Science, Osaka Prefecture University, Sakai, Osaka 599-8531, Japan

Received December 9, 2003; accepted January 10, 2004

In the previous X-ray crystallographic study, it was found that β-amylase from *Bacillus cereus* var. *mycoides* has three carbohydrate-binding sites aside from the active site: two (Site2 and Site3) in domain B and one (Site1) in domain C. To investigate the roles of these sites in the catalytic reaction and raw starch-binding, Site1 and Site2 were mutated. From analyses of the raw starch-binding of wild-type and mutant enzymes, it was found that Site1 contributes to the binding affinity to raw-starch more than Site2, and that the binding capacity is maintained when either Site1 or Site2 exists. The raw starch-digesting ability of this enzyme was poor. From inhibition studies by maltitol, GGX and α-CD for hydrolyses of maltopentaose (G5) and amylose ($\overline{DP}_n$ = 16) catalyzed by wild-type and mutant enzymes, it was found that α-CD is a competitive inhibitor, while, maltitol behaves as a mixed-type or competitive inhibitor depending on the chain length of the substrate and the mutant enzyme. From the analysis of the inhibition mechanism, we conclude that the bindings of maltitol and GGX to Site2 in domain B form an abortive ESI complex when amylose ($\overline{DP}_n$ = 16) is used as a substrate.

Key words: β-amylase, binding mechanism, binding site, inhibition, raw starch-binding.

Abbreviations: BCM, *Bacillus cereus* var. *mycoides*; CGTase, cyclodextrin glycosyltransferase; GGX, *O*-α-D-xylopyranosyl-(1-4)-*O*-α-D-glucopyranosyl-(1-4)-*O*-α-D-glucopyranoside; MBS, maltose-binding site; SBD, starch-binding-domain.

β-Amylase [EC 3.2.1.2] catalyzes the hydrolysis of α-1,4-glucosidic linkages of starch, and liberates β-anomeric maltose from the nonreducing ends of starch. It is an exo-acting enzyme with no activity towards α-1,6-glucosidic linkages, and is a member of family 14 of the sequence-based classification of glycoside hydrolases (*1*). β-Amylase is distributed in plants and microorganisms. Bacterial β-amylases have raw starch-binding ability owing to the C-terminal starch-binding-domain (SBD), which has homology with the SBDs of cyclodextrin glucosyltransferase (CGTase) and glucoamylase. The three-dimensional structures of β-amylases from plants (*2*) and *B. cereus* (*3–6*) have been reported. In the crystal structure of the catalytic site mutant E172A (Glu172→Ala) of β-amylase from *Bacillus cereus* var. *mycoides* (BCM β-amylase) complexed with maltopentaose (G5), we have found three saccharide-binding sites apart from the active site: Site1 in domain C and Site2 and Site3 in domain B (Fig. 1) (*4*). From the three-dimensional structures of β-amylase/GGX and β-amylase/maltose complexes, it is known that both GGX and maltose in substrate analogues bind to Site2 in domain B, which is about 30 Å away from the catalytic site (*6*). No saccharide binding at Site3 was observed in wild-type/maltose and wild-type/GGX complexes (*3*, *6*). This indicates that Site3 has less affinity for the ligand. Site2 does not show any similarity to the sac-

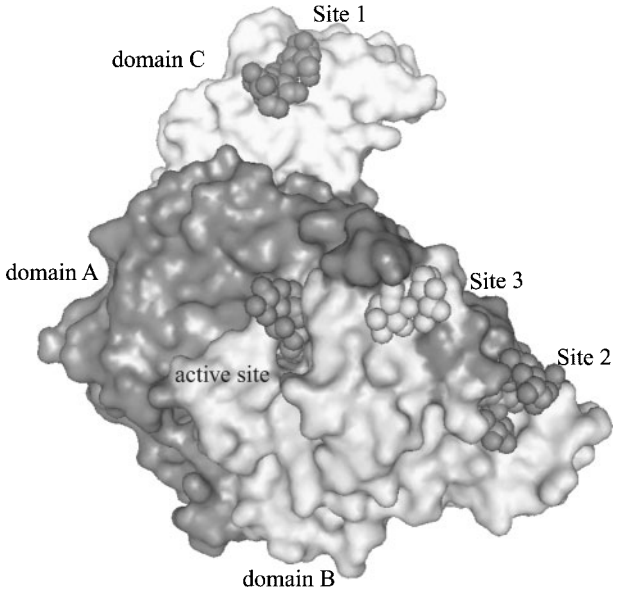

Fig. 1. **Surface model of the E172A-maltopentaose (G5) complex (pdb code 1ITC) using Pymol (http://www.pymol.org).** A sphere model represents G5, which binds to an active site and Sites 1–3. Three glucose residues from the non-reducing end of G5 are buried in the active site.

*Present address: Department of Life Sciences, Faculty of Bioresources, Mie University, 1515 Kamihama, Tsu, Mie 514-8507.
†To whom correspondence should be addressed. E-mail: nitta@biochem.osakafu-u.ac.jp

charide-binding sites of other amylases and is conserved only in bacterial β-amylases (*3*), but its function is unknown. Site1 in domain C shows structural similarity to maltose-binding site (MBS) 1 in SBD of CGTase (*8*) and glucoamylase (*9*), but the binding site corresponding to MBS2 in CGTase does not exit in β-amylase (*3*).

In the present study, to investigate the functions of Site1 and Site2, the raw starch-binding and digesting abilities of wild-type and mutant enzymes were analyzed quantitatively using various raw starches. Furthermore, the inhibitory effects of maltitol, GGX and α-CD on the hydrolysis of substrates with different chain lengths (*i.e.* G5 and amylose with $\overline{DP}_n$ = 16) were determined using wild-type and mutant enzymes. Taking the results of difference spectroscopic studies and evidence from X-ray crystallographic studies into consideration, the properties of the carbohydrate-binding sites (Site1 and Site2) are discussed.

MATERIALS AND METHODS

Media, Bacterial Strains and Plasmids—E. coli DH5α was used as the host strain for the manipulation of the BCM α-amylase gene. *E. coli* was grown at 37°C with shaking in Luria-Bertani medium [1% (w/v) polypepton/ 0.5% yeast extract/0.5% NaCl (pH 7.0)] supplemented with 100μg/ml ampicillin when appropriate. *E. coli* BL21(DE3), which was used as the host strain for expression, was grown in 2× YT medium [1.6% (w/v) polypepton/ 1% yeast extract/0.5% NaCl (pH 7.0)/1% glycerol] containing 100 μg/ml ampicillin. pET-21d was used as a cloning and sequencing vector. pHBCW, which bears the gene that codes for BCM β-amylase (*10*), was used as a template for PCR.

Site-Directed Mutagenesis and Expression of the BCM β-Amylase Gene—The full-length BCM β-amylase gene was amplified by PCR using the following primers: sense primer 5′-TGACCATGGCTGTAAATGGAAAAGGAA-3′ and antisense primer 5′-TTAAGCTTTTACCAACTTGTATG-AGA-3′, containing *Nco*I and *Hin*dIII restriction sites, respectively, at their 5′ ends. All mutations were made by a Quickchange™ site-mutagenesis kit (Stratagene) or the "megaprimer" method (*11*) using the following mutagenic primers: 5′-GTTCCCCATCGGCGGGTGGTAAAA-ATT-3′ for S235A; 5′-GTCTTTGCCGGCCATAGAAAGA-TATCC-3′ for Y249A; 5′-GGGAATCGCGCGGAATTAG-GAAGTNNYGACACAAAACAGTAGCC-3′ and 5′-CCCT-TAGCGCGCCTTAATCCTTCANNRCTGTGTTTTGTCAT-CGG-3′ for W449F; 5′-GGTACGGTTAAATCANNYCAA-ACAATACAACAAAGTTGGAATCC-3′ and 5′-CCATGCC-AATTTAGTNNRGTTTGATATGTTGTTTCAACCTTAGG-3′ for W495F; 5′-CCATATCCCCCCAAAAAAAATCAA-CTG-3′ for W51F. The reaction mixture of the Quick-change™ site-mutagenesis kit contained 50 ng of template DNA pHBCW, 20 pmol of each mutagenic primer, 0.2 mM of each dNTP and 2.5 units of *pfu* DNA polymerase in its recommended buffer. Amplification was obtained by 25 cycles of 60 s at 96°C, 60s at 60°C and 10 min at 72°C. The product was digested with *DPn*I at 37°C for 1 h to cut the parental supercoiled dsDNA, then transformed into *E. coli* XL1-Blue competent cells. W449F, W495F and W449F/W495F were made by this method. The other mutants (S235A, Y249A S235A/Y249A, W51F and quadruple mutant S235A/Y249A/W449F/W495F) were made by a megaprimer strategy. The first PCR was performed using the mutagenic primer and the sense or antisense primer. The cycling parameters were 25 cycles of 45 s at 94°C, 45 s at 55°C and 120 s at 72°C. The product was purified with a Geneclean II purification kit (Bio101, Inc.). The purified megaprimer product (200 ng) and 50 ng of template (pHBCW) were used for a second PCR step. After five cycles of Asymmetric PCR (*12*) were carried out with denaturation at 94°C for 1 min and extension at 72°C for 3 min, 20 pmol of the sense or antisense primer was added; the PCR cycling parameters were same as for the first PCR. The 1.5 kb product was purified by a Geneclean II kit, digested with the *Nco*I and *Hin*dIII of restriction enzymes and ligated into a pET21-d vector that had been digested with the same enzymes. All mutations were confirmed by DNA sequencing (Perkin Elmer, Inc.).

E. coli strain BL21 (DE3) was used for the production of wild-type BCM β-amylase and its mutants. BL21 (DE3) transformed with the appropriate vector was grown in 1 liter of 2× YT medium containing 100 μg/ml ampicillin and 1% glucose. The culture was shaken at 180 rpm. and 37°C until the optical density at 600 nm reached about 1.0. Then, 0.1 mM (final concentration) isopropyl-β-D-thiogalactopyranoside (IPTG) was added to the culture to induce the expression of BCM β-amylase, and cultivation was continued for a further 40 hours at 18°C.

Purification of Recombinant BCM β-Amylases—The cultivated cells were collected by centrifugation, washed once with sonication buffer [1 mM EDTA in 50 mM sodium phosphate buffer (pH 7.0)], resuspended in the same buffer containing 1mg lysozyme per g cells, and disrupted by sonication with an ultrasonic disrupter. The soluble fraction of disrupted cells was extracted by centrifugation (4°C, 10,000 ×*g*, 15 min). Ammonium sulfate was added to the extract to achieve 15% saturation, and the resulting supernatant was applied to a column of phenyl-TOYOPEARL 650M (Tosoh Co.) equilibrated with 15% saturated ammonium sulfate in 50 mM sodium phosphate buffer (pH 7.0). The column was washed with 300 ml of the same buffer and eluted. The resulting protein fraction was dialyzed against 50 mM Tris-HCl buffer (pH 9.0) and loaded onto a column of DEAE-TOYOPE-ARL 650S (Tosoh Co.) equilibrated with the same buffer. After washing with the same buffer, the protein was eluted with a linear gradient from 0 to 70 mM NaCl in the same buffer. The protein fractions were collected, desalted and concentrated in a Centriprep (Amicon, 30 kDa cut-off filter). The purity of the enzyme preparation was examined by polyacrylamide gel electrophoresis (7.5%, pH 8.9) (PAGE) and SDS/PAGE (10%, pH 8.8) (*13*) using Coomassie Brilliant Blue R-250 as a stain; a rabbit anti-β-amylase polyclonal antibody was used for western blotting. The concentrations of the pure wild-type and mutant β-amylases were calculated from the absorbance at 280 nm, using an absorbance of 20.8 at 280 nm for a 1% solution ($A^{1\%}_{280}$) and M_r = 58,300 for the wild-type enzyme and S235A. The concentration of each mutant protein was calculated by the same method, using $A^{1\%}_{280}$ values calculated from the amino acid compositions (*14*). The values were 20.6 for Y249A and S235A/Y249A, 19.9

for W449F and W495F, 19.2 for W449F/W495F and 19.0 for the quadruple mutant.

Determination of Amino Acid Sequences—The N-terminal amino acid sequences of the mutant enzymes were analyzed by a gas-phase protein sequencer (Shimadzu PSQ-1).

Measurements of CD and Difference Spectra—The CD and difference spectra were measured at pH 7.0 and 25°C (25 mM sodium phosphate buffer). The CD spectra of the wild-type and mutant enzymes were obtained with a J-720 spectropolarimeter (Jasco Co.) using a protein concentration of 3 μM. All spectra were recorded from 190 to 260 nm. Difference spectra from 260 to 320 nm were measured at pH 7.0 and 25°C (25 mM sodium phosphate buffer) with a UV-1600PC recording spectrophotometer (Shimazu Co.).

Enzyme Reaction—Reactions were performed at 25°C and pH 7.0 (25 mM sodium phosphate) and the amount of reducing sugar liberated in the reaction mixture with time was determined by a modification of the method of Somogyi-Nelson (*15*). The reaction velocity was obtained from the initial slope of the reaction curve. Maltopentaose (G5) and amylose with a number-average degree of polymerization ($\overline{DP}_n$) of 16 were used as substrates. Cyclohexaamylose (α-CD), maltitol and *O*-α-D-glucopyranosyl-(1→4)-*O*-α-D-glucopyranosyl-(1→4)-D-xylopyranose (GGX) were used as inhibitors. GGX was synthesized by the method previously reported (*16*). The substrates and inhibitors, except GGX, were products of Hayashibara Biochemical Laboratories, Inc. (Japan).

Binding Assay to Raw Starch—Raw wheat, potato, sweet potato and corn starches (Wako Pure Chemical Industries, Ltd.) were washed with water to remove the soluble fraction completely, and then centrifuged and dried. The binding of the enzyme to raw corn starch was measured at 4°C and pH 7.0 (50 mM sodium phosphate). Wild-type or mutant enzyme was mixed with a suspension of raw corn starch, with the concentration of the raw starch fixed at 100 mg/ml and the enzyme concentration varied from 0.8 to 16 μM. After incubation with gentle shaking for 1 h at 4°C and pH 7.0 (50 mM sodium phosphate), the mixture was centrifuged at 15,000 ×*g* for 10 min, and the remaining enzyme activity (initial velocity) of the supernatant was measured using 1% soluble starch as a substrate. The enzyme activity was obtained by measuring the initial velocity of the hydrolytic reaction.

Degradation of Raw Starch—Reaction mixtures containing raw starch (wheat, corn, potato or sweet potato) and enzyme were incubated at 25°C for 24 h under gently shaking. For these experiments, the final concentrations of enzyme and raw starch were fixed at 1 mg/ml and 5%, respectively. The solvents used were phosphate buffer (pH 7.0) for β-amylase and pullulanase and acetate buffer (pH 5.4) for Taka-amylase A. The concentration of reducing sugar in the supernatant was measured by a modification of the method of Somogyi-Nelson (*15*).

RESULTS AND DISSCUSSIONS

Physicochemical Properties of the Recombinant Enzymes—SDS-PAGE, native PAGE, and Western-blotting of the wild-type and mutant enzymes (S235A, Y249A, S235A/Y249A, W449F/W495F and S235A/Y249A/W449F/W495F) were performed. From the results, it was found that all recombinant enzymes were purified to homogeneity as determined both electrophoretically and immunologically. The mutant enzymes showed different mobilities in native PAGE compared with wild-type enzyme due to the substitution of one or more amino acid residues. The sequences of N-terminal five amino acids of the mutant enzymes were the same as that of the wild-type enzyme (AVNGK). The CD spectra of the wild-type and mutant enzymes were the same (data not shown), indicating that the secondary structures of all recombinant enzymes are the same.

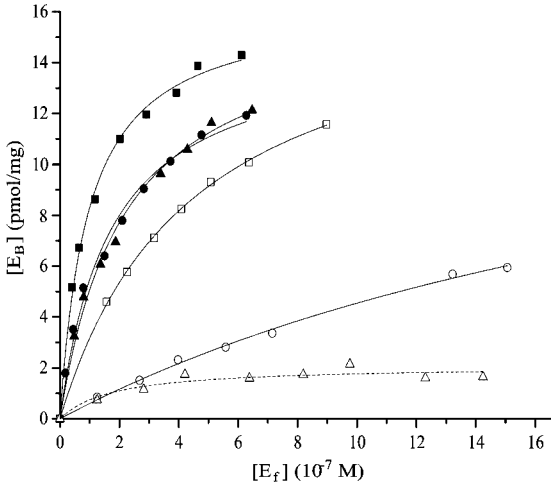

Fig. 2. **Binding isotherms of enzymes to raw corn starch at pH 7.0 and 4°C: wild-type enzyme (solid squares), S235A (solid circles), Y249A (solid triangles), S235A/Y249A (open squares), W449F/W495F (open circles) and S235A/Y249A/W449F/W495F (open triangles).** The solid lines represent the best-fit curves obtained by the nonlinear least-squares method.

Evaluation of Raw Starch-Binding Ability—The amount of adsorption (or binding ability) of the wild-type enzyme to raw starch at pH 7.0 was almost the same irrespective of origin, *i.e.*, wheat, corn, sweet potato or potato (results not shown). In the present study, we used raw corn starch, because over 95% of the enzyme bound to the raw corn starch within the equilibration time of 30 min at pH 7.0 and 4°C in reaction mixtures containing 1.6 μM enzyme and 10% raw starch. This implies that the wild-type enzyme has a high affinity for raw corn starch, and the binding ability is comparable to that of CGTase (*17*).

The binding abilities of the wild-type and mutant enzymes to raw corn starch were analyzed at pH 7.0 and 4°C and the results were evaluated according to Langmuir's adsorption isotherm (Eq. 1).

$$[E_B] = \frac{E_{Bmax}[E_f]}{K_d + [E_f]} \quad (1)$$

in which $[E_f]$ is the concentration of unbound enzyme, $[E_B]$ is the amount of enzyme bound to the raw corn starch, E_{Bmax} is the maximal amount of enzyme bound to the raw corn starch and K_d is the reciprocal of the adsorption equilibrium constant. $[E_f]$ was calculated from the enzyme activity in the supernatant of the reaction mixture, and $[E_B]$ was obtained by subtracting the amount of unbound enzyme from the total amount of enzyme. The

Table 1. **Binding parameters of the wild-type and mutant enzymes to raw corn starch at pH 7.0 and 4°C.**

Enzyme	E_{Bmax} (pmol/mg)	K_d (μM)	$-\Delta G°$ (kJ/mol)	$\Delta(-\Delta G°)^b$ (kJ/mol)
wild-type	16.1 ± 0.4	0.094 ± 0.007	37.2 ± 0.1	–
S235A	15.1 ± 0.7	0.172 ± 0.021	35.9 ± 0.1	1.3
Y249A	16.2 ± 0.7	0.219 ± 0.023	35.3 ± 0.1	1.9
S235A/Y249A	17.0 ± 0.3	0.445 ± 0.015	33.7 ± 0.1	3.5
W449F	15.8 ± 1.3	2.14 ± 0.18	30.1 ± 0.1	7.1
W495F	16.4 ± 1.7	2.08 ± 0.37	30.1 ± 0.2	7.1
W449F/W495F	16.7 ± 1.8	2.34 ± 0.21	29.8 ± 0.1	7.3
quadruple mutant[a]	1.9 ± 0.1	0.18 ± 0.04	35.7 ± 0.2	–

[a]Quadruple mutant: S235A/Y249A/W449F/W495F. [b]$\Delta(-\Delta G°) = (-\Delta G°_{wild\text{-}type}) - (-\Delta G°_{mutant})$.

plots of $[E_B]$ versus $[E_f]$ for the wild-type and mutant enzymes are shown in Fig. 2. Each plot was fitted to equation 1 by the nonlinear least-squares method, and the obtained values of K_d and E_{Bmax} are listed in Table 1.

The E_{Bmax} values of all enzymes were almost the same except for the quadruple mutant enzyme, S235A/Y249A/W449F/W495F. This suggests that the enzymes, except the quadruple mutant enzyme, bind to raw starch with the same binding mode. The E_{Bmax} of the quadruple mutant enzyme (1.9 pmol/mg) is about 1/8 that of the other enzymes, although the K_d value (0.18 μM) is nearly equal to that of S235A. The remarkable change in E_{Bmax} suggests that the binding mode of the quadruple mutant enzyme differs from that of the wild-type and other mutant enzymes.

Raw Starch-Binding at Site2 in Domain B—Maltose binds to Site2 of the wild-type enzyme through van der Waal's contacts and one hydrogen bond with Tyr249, and two hydrogen bonds with Ser235. This site is conserved only in bacterial β-amylases (*3*) and is not similar to the saccharide-binding sites of other amylases. By mutation of Tyr249 and/or Ser235 at Site2, the E_{Bmax} values were not affected but the K_d values increased compared with the wild-type enzyme. If it is assumed that the raw starch represents a solid state and has equivalent and independent binding sites to which the enzyme binds, the standard Gibb's free energy change of binding between enzyme and binding sites on raw starch, $-\Delta G°$, is obtained from the K_d value. The values are listed in Table 1, together with the difference in $-\Delta G°$ between mutant and wild-type enzymes, $\Delta(-\Delta G°)$. Compared with the wild-type enzyme, the decrease in binding affinity of S235A, $\Delta(-\Delta G°)$, was 1.3 kJ mol^{-1}, which may correspond to the loss of two hydrogen bonds with glucose residue at Site2. Fersht, A.R. *et al*. (*18*) and Street, I.P. *et al*. (*19*) have reported that the Gibb's free energy change of a hydrogen bond in water is generally somewhere between 2.1 and 6.3 kJ mol^{-1}. Compared with those values, the value of $\Delta(-\Delta G°)$ for S235A is rather small. However, the present results support the results of a study on hydrogen bonding in the interaction between a xylan binding module and xylan by Xie, H *et al*. (*20*), who concluded that hydrogen bonding contributes little to specificity or affinity when the ligand is bound to the exposed surface of the enzyme. In the case of Y249A, the $\Delta(-\Delta G°)$ was 1.9 kJ mol^{-1}, which corresponds to a loss of hydrophobic binding energy. In the case of the double mutant S235A/Y249A, the value was 3.5 kJ mol^{-1}, which is nearly equal to the sum of the values for S235A and Y249A. This implies that both residues contribute independently to the binding. Thus, we conclude that Site2 in domain B is involved in raw starch-binding of this enzyme.

Raw Starch-Binding at Site1 in Domain C—Maltose or a maltose unit of maltooligosaccharide binds to Trp449 and Trp495 at the Site1 in domain C through van der Waal's contacts between their indole groups and the glucopyranose rings (*3*, *4*, *6*). In the absence of the Trp449 or Trp495 indole group, the K_d value of the mutant enzyme increased to about 2.1 μM, which is nearly equal to that of the double mutant W449F/W495F. The loss of binding affinity is 7.1–7.3 kJ/mol. Thus, the contribution of Site1 to the binding affinity is about two times as large as that of Site2; thus, Site1 is more important for binding to raw starch than Site2. Many cellulose-binding modules contain Trp residues, and Nagy, T. *et al*. (*21*) have reported that the lack of one Trp residue causes a reduction in binding energy of about 8.4 kJ mol^{-1}. From a study of the carbohydrate-binding module of xylanase 10A, it is known that the $\Delta(-\Delta G°)$ value of Trp residue variants are 6–8 kJ mol^{-1} (*22*). The $\Delta(-\Delta G°)$ value of W449F/W495F is within this range, and the lack of either Trp residue causes a total loss of the binding affinity of Site1. On the other hand, the E_{Bmax} of W449F/W495F does not differ from that of the wild-type enzyme. This indicates that the binding capacity to raw corn starch does not change while the binding ability of either Site1 or Site2 remains.

Degradation of Raw Starch—The raw starch-digesting abilities of the wild-type and mutant enzymes were examined using various raw starches (wheat, corn, potato and sweet potato), and with Taka-amylase A, which scarcely adsorbs to raw starches and digests them, as negative control. The results for the raw corn starch are listed in Table 2. The replacement of amino acids at both sites reduced the hydrolytic activity compared with the wild-type enzyme. Similar results were obtained for the other raw starches. As β-amylase cannot cleave α-1,6-glucosidic linkages, the hydrolysis of raw starch stops at α-1,6-glucosidic linkage. Therefore, pullulanase was added to the mixture of β-amylase and raw starch in order to hydrolyze the linkages to allow the degradation to proceed. However, no significant effect was observed (data not shown). From these results, it was found that BCM β-amylase hardly hydrolyzes raw starch, although it binds to it strongly. Other amylases with binding ability to raw starch degrade the starch, so the behavior of this enzyme is uncommon.

BCM β-amylase is composed of two functional domains, a catalytic domain (domains A and B) and starch-binding domain (domain C). When these functional domains are expressed separately in *E.coli*, they lose both their hydro-

Table 2. **Digestion of raw corn starch by the wild-type and mutant enzymes at pH 7.0 and 25°C.**

Enzyme	Liberated reducing sugar (mM)	Relative digesting ability (%)
Taka-amylase A[a]	3.12	100
wild-type	1.25	40
S235A/Y249A	0.61	20
W449F/W95F	0.65	21
quadruple mutant[b]	0.43	14

[a]Negative control for the digestion of raw corn starch. [b]Quadruple mutant: S235A/Y249A /W449F/W495F.

lytic activity and raw starch-binding ability (unpublished data), which implies that the structure and function of each domain are maintained through interdomain interactions between the two domains. On the other hand, the functional domains of glucoamylase maintain their original functions when expressed independently (*23*), and SBD of CGTase is also independent of catalytic domain (*24*).

In thinking about the reason why BCM β-amylase cannot digest raw starch, it is noted that exo-acting amylases such as glucoamylase bind mainly at one point in the raw starch and yield products successively from the ends of the starch (*25*). However, in β-amylase, there is no structural flexibility, such as a linker region of glucoamylase between the catalytic domain and domain C. The SBD of CGTase and glucoamylase have two maltose-binding sites (MBS1 and MBS2) with different functions and binding constants. Recent work has revealed that MBS2 of CGTase has a role in guiding the substrate into the groove loading to the active site (*17*), and that the SBD of glucoamylase can disrupt the raw starch structure through the structural change of MBS2 (*26*). However, a site corresponding to MBS2 is not found in β-amylase. Second, BCM β-amylase hydrolyzes raw starch to liberate maltose, but the binding of maltose to Site1 and/or Site2 makes the raw starch-enzyme complex dissociate. The concentration of maltose liberated from raw corn starch by wild-type β-amylase was 1.25 mM (Table 2), but 10 mM maltose is necessary to release the enzyme from raw starch completely. Thus, this possibility is excluded. The third possibility is that BCM β-amylase can disrupt the structure of raw starch, but that hydrolysis stops at the α-1,6-glucosidic linkages in the starch. As described above, the digestion of raw starch did not proceed when pullulanase was added to the reaction mixture. So, this possibility is excluded as well. As a result, it is concluded that the poor raw starch-digesting ability of BCM β-amylase arises from a lack of structural flexibility between catalytic domain and domain C, and from the structure of domain C without second MBS.

Difference Spectrum Analysis—In X-ray crystallographic studies of this enzyme, Oyama (*7*) found that an α-CD binds only to the active site (subsites +2 and +3 in Fig. 3). Five amino acid residues of the MBS1 of CGTase are conserved in Site1 of β-amylase and have similar locations and orientations. This implies that α-CD could bind to Site1 in similar manner to CGTase (*3*, *7*). We measured the difference spectrum to examine whether α-CD binds to Site1 or not. As shown in Fig. 4A, the difference spectrum of the wild-type enzyme induced by α-CD shows two peaks at 287 nm and 298–299 nm due to Trp residues. The difference spectra of W449F/W495F (mutated Site1) and S235A/Y249A (mutated Site2) induced by α-CD show no significant differences compared to the wild-type enzyme. This indicates that the binding of α-CD to subsites +2 and +3 causes a perturbation of the environment around Trp293, yielding two peaks at 287 nm and 298–299 nm in the difference spectrum. Thus, it is concluded that α-CD binds to subsites +2 and +3 in the active site but not to Site1 and Site2.

As shown in Fig. 4B, the difference spectra of the wild-type enzyme, S235A/Y249A and W449F/W495F (data not shown) induced by maltitol show a single peak at 293 nm due to a Trp residue, but there is no significant difference among them. The difference spectrum of W51F shows no peaks: the peak at 293 nm disappears completely. When maltose instead of maltitol was used as a ligand, the same results were obtained. This indicates that when a

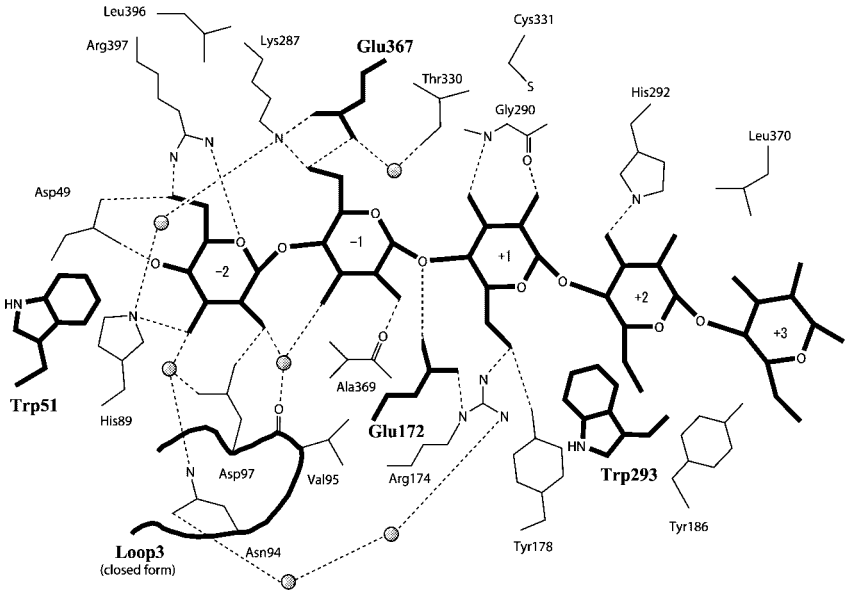

Fig. 3. **Hypothetical binding manner of maltopentaose (G5) in the active site of BCM β-amylase.** Numbers (–2 to +3) on the glucopyranose of G5 indicate subsite numbers, and the non-reducing end of G5 occupies subsite –2. The catalytic residues (Glu172 and Glu367), two Trp residues (Trp51 and Trp293) and G5 are drawn with heavy lines.

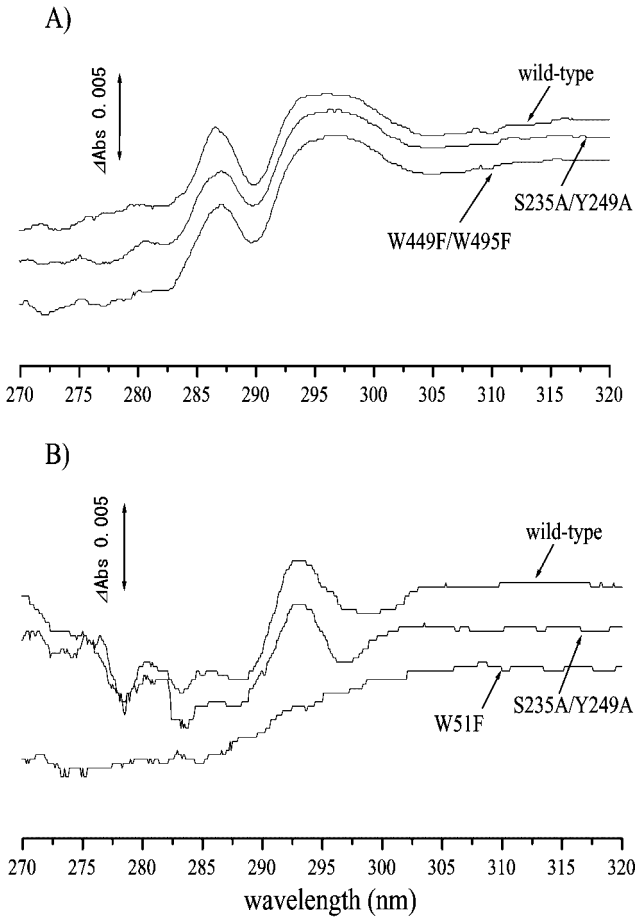

Fig. 4. **Difference spectra of wild-type and mutant enzymes induced by α-CD and maltitol at pH 7.0 and 25°C: (A) spectra induced by α-CD (15 mM); (B) spectra induced by maltitol (10 mM).** Enzyme concentration was 10 μM.

ligand such as maltitol or maltose binds to subsites –1 and –2 (Fig. 3), the environment of Trp51 is perturbed to produce a difference spectrum with a peak at 293 nm (see Fig. 4B).

Hydrolysis of Soluble Substrate—To investigate whether Site1 and Site2 are involved in the substrate hydrolysis or not, the kinetic parameters of the hydrolysis of a soluble substrate by the wild-type and mutant enzymes were determined and the results are shown in Table 3. For all enzymes, the Michaelis constant, K_m, of amylose ($\overline{DP}_n$ = 16) is almost the same. This indicates that the binding affinity of the substrate to the enzyme is not affected by mutations at Site1 and/or Site2. On the other hand, the values of molecular activity, k_0, for the mutant enzymes decreased to 50–70% of the wild-type enzyme, and the catalytic efficiencies of S235A/Y249A and S235A/Y249A/W449F/W495F toward amylose ($\overline{DP}_n$ = 16) and soluble starch were about half those of the wild-type enzyme. The result for β-amylase is opposite to the result of CGTase, for which k_0 does not change and K_m increases by mutation of the MBS (*17*). In the case of BCM β-amylase, the mutation of carbohydrate-binding sites does not cause a decrease in the binding affinity to the substrate, and, therefore, it is suggested that the sites play no role in the enhancement of the local substrate concentration.

For β-amylase, we will try to explain the above result based on the subsite theory (*27*). When productive and nonproductive binding modes are considered, k_0 and K_m are expressed as follows.

$$k_0 = k_{int}\frac{\Sigma K_p}{\Sigma K_p + \Sigma K_q} \quad (2)$$

$$\frac{1}{K_m} = \Sigma K_p + \Sigma K_q \quad (3)$$

where k_{int} is the intrinsic rate constant of the α-1,4-glucosidic bond cleavage, and is independent of the chain length of the maltooligosaccharide. ΣK_p and ΣK_q are the total association constants of the productive and nonproductive binding modes, respectively. As the K_m values of β-amylase do not vary, the sum of ΣK_p and ΣK_q is constant (Eq. 3). From equation 2, the following two cases are conceivable: (1) k_{int} is invariable and the decrease in k_0 is caused by the decrease in the $\Sigma K_p/\Sigma K_q$ ratio; (2) k_{int} of the mutant enzyme decreases and $\Sigma K_p/\Sigma K_p + \Sigma K_q$ is invariable. In the latter case, mutation(s) at Site1 and/or Site2 cause a change in the environment of the catalytic residues, although the two sites are located 30 Å away from active site. Case 1 is supported by the fact that the binding affinity for the productive binding mode is decreased by mutations at Site1 and Site2, a result obtained from the inhibition study described below.

Inhibition by Maltitol, α-CD and GGX—The inhibition experiments were performed at 25°C and pH 7.0 using maltopentaose (G5) and amylose ($\overline{DP}_n$ = 16) as substrates. When G5 was used as a substrate, the Lineweaver-Burk plots of the inhibition of hydrolysis of the wild-type enzyme by maltitol showed straight lines that intersected at a single point on the vertical axis (results not shown). This indicates that the inhibition by maltitol is competitive. Also, the Dixson plot shows a straight line, indicating one molecule of maltitol participates in

Table 3. **Kinetic parameters of wild-type and mutant enzymes for hydrolytic activity at pH 7.0 and 25°C.**

	Amylose[b]			Soluble starch
Enzyme	k_0 (s^{-1})	K_m (mM)	k_0/K_m (s^{-1} mM^{-1})	Relative activity (%)
wild-type	1,100 ± 40	0.72 ± 0.08	1,510 ± 170	100
S235A	1,060 ± 50	0.70 ± 0.09	1,470 ± 180	88
Y249A	1,040 ± 40	0.71 ± 0.07	1,400 ± 140	80
S235A/Y249A	730 ± 30	0.65 ± 0.07	1,100 ± 130	63
W449F/W495F	580 ± 40	0.61 ± 0.06	950 ± 140	61
quadruple mutant[a]	450 ± 30	0.60 ± 0.06	740 ± 80	51

[a]Quadruple mutant: S235A/Y249A/W449F/W495F. [b]Amylose with $\overline{DP}_n$ = 16.

Table 4. **Inhibitions by substrate analogs for wild-type and mutant enzyme catalyzed reactions at pH 7.0 and 25°C.**

Inhibitor	Enzyme	Substrate	K_i (mM)	K_i' (mM)	Inhibition type
α-CD	wild-type	amylose[b]	0.8 ± 0.1	–	competitive
maltitol	wild-type	G5	3.1 ± 0.2	–	competitive
maltitol	S235A/Y249A	amylose[b]	5.1 ± 0.9	–	competitive
maltitol	quadruple mutant[a]	amylose[b]	5.7 ± 0.7	–	competitive
maltitol	wild-type	amylose[b]	2.8 ± 0.3	21 ± 4	mixed-type
GGX	wild-type	amylose[b]	0.45 ± 0.19	0.72 ± 0.31	mixed-type

[a]Quadruple mutant: S235A/Y249A/W449F/W495F. [b]Amylose with $\overline{DP}_n$ = 16.

the inhibition. The results are listed in Table 4. On the other hand, when amylose ($\overline{DP}_n$ = 16) was used as the substrate, the plots of the inhibition by maltitol also showed straight lines, but they intersected at different points on the vertical axis, as shown in Fig. 5A. The secondary plots of the slope and intercept on the vertical axis showed straight lines (Figs. 5, B and C). These results indicate that the inhibition by maltitol is a mixed type and also that one molecule of maltitol relates to the inhibition. Thus, it was found that the type of inhibition by maltitol varies depending on the chain length of the substrate.

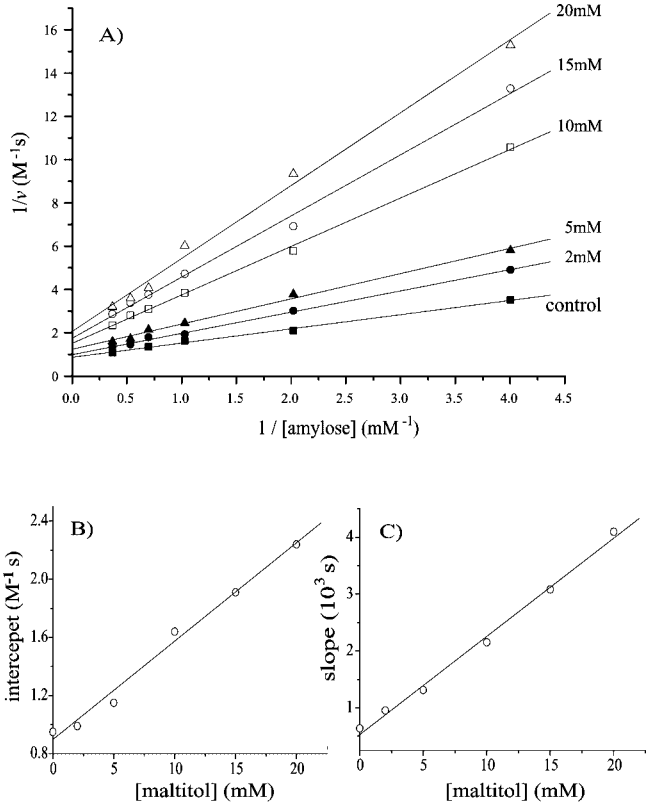

Fig. 5. **(A) Lineweaver-Burk plot of mixed type inhibition by maltitol of the wild-type enzyme catalyzed hydrolysis of amylose ($\overline{DP}_n$ = 16) at pH 7.0 and 25°C.** The reaction was carried out in the absence (solid squares) and in the presence of maltitol at concentrations of 2 mM (solid circles), 5 mM (solid triangles), 10 mM (open squares), 15 mM (open circles) and 20 mM (open triangles). The concentration of wild-type enzyme was 2 nM. **(B) The plot of intercept versus concentration of maltitol obtained from plot A. (C) The plot of slope *versus* concentration of maltitol obtained from plot A.**

For the mixed type inhibition mechanism, the following two models are considered (*28*): a random type (Scheme A), and a mixed type including competitive and uncompetitive inhibitions (scheme B) (Fig. 6). In the case of the inhibition by maltitol, a Scheme B mechanism is conceivable, while Scheme A is excluded because maltitol can bind to the active site. The rate equation for Scheme B is expressed as follows:

$$v = \frac{V \cdot s}{K_m\left(1 + \frac{i}{K_i}\right) + s\left(1 + \frac{i}{K_i'}\right)} \quad (4)$$

This is rewritten as

$$\frac{1}{v} = \left(\frac{K_m}{V} + \frac{K_m}{VK_i}i\right)\frac{1}{s} + \left(\frac{1}{V} + \frac{1}{VK_i'}i\right) \quad (5)$$

where v, s and i are the initial velocity and the concentrations of substrate and inhibitor, respectively. V, K_i and K_i' represent maximum velocity and inhibitor constants, respectively. According to equation 4, the K_i and K_i' values of maltitol for the hydrolysis of amylose ($\overline{DP}_n$ = 16) by the wild-type enzyme were determined using the nonlinear least-squares method, and these are listed in Table 4. Next, assuming that Site1 or Site2 is a binding site other than the active site, the inhibition experiment of the hydrolysis of amylose ($\overline{DP}_n$ = 16) by maltitol was performed for the mutant enzymes S235A/Y249A and S235A/Y249A/W449F/W495F. The Lineweaver-Burk plots of the inhibition are shown in Fig. 7. The results indicate that inhibitions of hydrolysis of both mutant enzymes by maltitol are competitive, although the wild-type shows a mixed type inhibition. These results are also listed in Table 4. Thus, it is concluded that the mutant enzymes

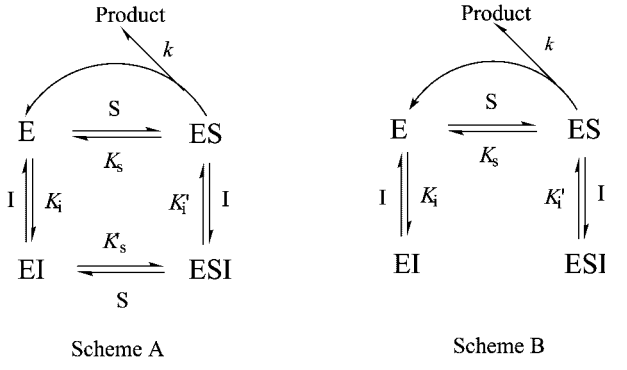

Fig. 6. **Mixed-type inhibition scheme: (A) random type model (B) mixed-type model comprising competitive and uncompetitive inhibitions.**

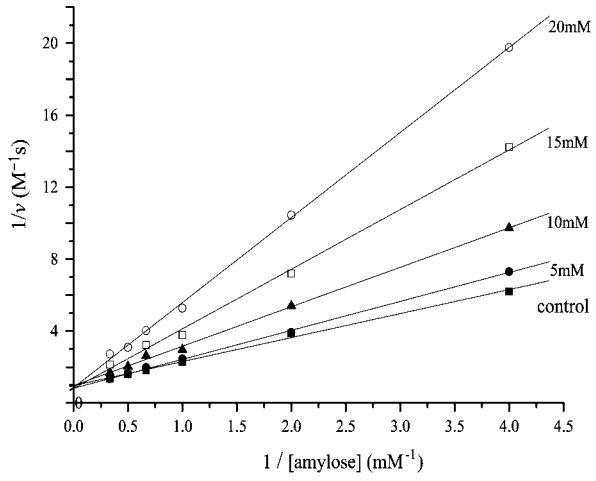

Fig. 7. **Lineweaver-Burk plot of competitive inhibition by maltitol for S235A/Y249A/W449F/W495F catalyzed hydrolysis of amylose ($\overline{DP}_n$ = 16) at pH 7.0 and 25°C.** The reaction was carried out in the absence (solid squares) and in the presence of maltitol at concentrations of 5 mM (solid circles), 10 mM (solid triangles), 15 mM (open squares) and 20 mM(open circles). The concentration of the mutant enzyme used was 4 nM.

lose their ability to bind maltitol at Site2, so that the abortive ESI complex in scheme B is not formed and the inhibition changes to a competitive type. Thus we conclude that maltitol inhibits hydrolysis according to the mechanism of scheme B.

The K_i values of maltitol for S235A/Y249A and S235A/Y249A/W449F/W495F are about twice that for the wild-type enzyme. This suggests that a mutation at Site2 causes the decrease in the affinity (1.5–1.8 kJ/mol) for the productive binding of substrate, because maltitol can bind to subsites –1 and –2. The results support the hypothesis that the decrease in the $\Sigma K_p/\Sigma K_q$ ratio caused by mutations at Site1 and Site2 results in the invariable K_m and the decrease in k_0 for the hydrolysis of amylose ($\overline{DP}_n$ = 16).

The inhibitory effect of α-CD on the hydrolysis of the amylose ($\overline{DP}_n$ = 16) catalyzed by the wild-type enzyme was examined by the same method (data not shown). The inhibition type and K_i are listed in Table 4. In contrast to maltitol, the inhibition by α-CD is competitive. X-ray crystallographic analysis of the wild-type enzyme complexed with α-CD has revealed that α-CD binds only to the subsites +2 to +3, with no α-CD binding observed at Site2 (*7*). So, the results of the inhibition by α-CD are consistent with the results of X-ray crystallographic analysis.

GGX is a compound in which the reducing end glucose of maltotriose is replaced by D-xylose. From X-ray crystallographic studies (*6*), we have found that two molecules of GGX bind to the enzyme, one to subsites +1 to +3 and another to Site2. The inhibition by GGX is a mixed-type for the hydrolysis of amylose ($\overline{DP}_n$ = 16) catalyzed by wild-type enzyme (data not shown). So, the mixed-type inhibition of GGX can be understood by the mechanism of scheme B. The inhibitor constants are listed in Table 4. Thus, Scheme B explains the mechanisms of the mixed-type inhibition by maltitol and GGX. K_i and K_i' are the dissociation constants for the EI complex in the active site and ESI complex at Site2, respectively. The K_i values of GGX and maltitol are 0.45 mM and 2.8 mM, respectively. The binding affinity of GGX to subsites +1 to +3 is larger than that of maltitol to subsites –1 and –2. On the other hand, in the three-dimensional structures of β-amylase complexed with GGX and maltose, the two glucose residues of GGX or maltose at Site2 have the same interaction with the enzyme, and the xylose ring of GGX interacts with Gln239 and Asn243 through hydrogen bonds (*6*), implying that the binding affinity of GGX to Site2 is larger than that of maltose. In addition, the open-ring structure of the reducing end of maltitol may further decrease the binding affinity to Site2. This explains why the K_i' value of maltitol is 30 times larger than that of GGX.

In previous X-ray crystallographic studies of enzyme-ligand complexes, we observed that the non-reducing ends of sugars bound to sites other than the active site do not directly face to the active cleft (*4*, *6*). As β-amylase catalyzes the hydrolysis of starch from the non-reducing end, it is implied that the binding sites do not play the important role observed for MBS2 in CGTase, which is considered to guide the substrate into the groove loading to the active site (*17*). In the present study, we found the additional fact that an inhibitor (substrate analogue) forms an abortive ESI complex by binding at Site2, thus affecting the catalytic action of the enzyme when a long chain-length substrate is used. We conclude that Site2 is involved in the hydrolysis of amylose catalyzed by BCM β-amylase, although the particular role of the site remains unknown.

We thank Hayashibara Biochemical Laboratories, Inc. for donating the various saccharides.

REFRENCES

1. Henrissat, B. and Davis, G. (1997) Structural and sequence-based classification of glycoside hydrolases. *Curr. Opin. Struct. Biol.* **7**, 637–644
2. Mikami, B., Hehre, E.J., Sato, M., Katsube, Y., Hirose, M., Morita, Y., and Sacchettini, J.C. (1993) The 2.0-Å resolution structure of soybean β-amylase complexed with α-cyclodextrin. *Biochemistry* **32**, 6836–6845
3. Mikami, B., Adachi, M., Kage, T., Sarikaya, E., Nanmori, T., Shinke, R., and Utsumi, S. (1999) Structure of raw starch-digesting *Bacillus cereus* β-amylase complexed with maltose. *Biochemistry* **38**, 7050–7061
4. Miyake, H., Kurisu, G., Kusunoki, M., Nishimura, S., Kitamura, S., and Nitta, Y. (2003) Crystal structure of a catalytic site mutant of β-amylase from *Bacillus cereus* var. *mycoides* cocrystallized with maltopentaose. *Biochemistry* **42**, 5574–5581
5. Oyama, T., Kusunoki, M., Kishimoto, Y., Takasaki, Y., and Nitta, Y. (1999) Crystal structure of β-amylase from *Bacillus cereus* var. *mycoides* at 2.2 Å resolution. *J. Biochem.* **125**, 1120–1130
6. Oyama, T., Miyake, H., Kusunoki, M., and Nitta, Y. (2003) Crystal structures of β-amylase from *Bacillus cereus* var *mycoides* in complexes with substrate analogs and affinity-labeling reagents. *J. Biochem.* **133**, 467–474
7. Oyama, T. (1999) Doctoral thesis of Osaka Prefecture University, Japan
8. Lawson, C.L., van Montfort, R., Strokopytov, B., Rozeboom, H.J., Kalk, K.H., de Vries, G.E., Penninga, D., Dijkhuizen, L., and Dijkstra, B.W. (1994) Nucleotide sequence and X-ray structure of cyclodextrin glycosyltransferase from *Bacillus cir-*

culans strain 251 in a maltose-dependent crystal form. *J. Mol. Biol.* **236**, 590–600
9. Sorimachi, K., Jacks, A.J., Le Gal-Coeffet, M.F., Williamson, G., Archer, D.B., and Williamson, M.P. (1996) Solution structure of the granular starch binding domain of glucoamylase from *Aspergillus niger* by nuclear magnetic resonance spectroscopy. *J. Mol. Biol.* **259**, 970–987
10. Yamaguchi, T., Matsumoto, Y., Shirakawa, M., Kibe, M., Hibino, T., Kozaki, S., Takasaki, Y., and Nitta, Y. (1996) Cloning, sequencing, and expression of a β-amylase gene from *Bacillus cereus* var. *mycoides* and characterization of its products. *Biosci. Biotechnol. Biochem.* **60**, 1255–1259
11. Sarkar, G. and Sommer, S.S. (1990) The "megaprimer" method of site-directed mutagenesis. *Biotechniques* **8**, 404–407
12. Datta, A.K. (1995) Efficient amplification using 'megaprimer' by asymmetric polymerase chain reaction. *Nucleic Acids Res.* **23**, 4530–4531
13. Laemmli, U.K. (1970) Cleavage of structural proteins during the assembly of the head of bacteriophage T_4. *Nature* **227**, 680–685
14. Pace, C.N., Vajdos, F., Fee, L., Grimsley, G., and Gray , T. (1995) How to measure and predict the molar absorption coefficient of a protein. *Protein Sci.* **4**, 2411–2423
15. Hiromi, K., Takasaki, Y., and Ono, S. (1963) Kinetic of hydrolytic reaction catalyzed by crystalline bacterial α-amylase. *Bull. Chem. Soc. Jpn.* **36**, 563–569
16. Takeo, K., Teramoto, Y., Shimono, Y., and Nitta, Y. (1991) Synthesis of the oligosaccharides α-D-Glc*p*-(1→4)-D-Xyl*p*, -α-D-Xyl*p*-(1→4)-D-Glc*p*, α-D-Glc*p*-(1→4)- α-D-Glc*p*-(1→4)-D-Xyl*p*, α-D-Glc*p*-(1→4)- α-D-Xyl*p*-(1→4)-D-Glc*p*, α-D-Xyl*p*-(1→4)-α-D-Glc*p*-(1→4)-D-Glc*p*. *Carbohydr. Res.* **209**, 167–179
17. Penninga, D., van der Veen, B.A., Knegtel, R.M., van Hijum, S.A., Rozeboom, H.J., Kalk, K.H., Dijkstra, B.W., and Dijkhuizen, L. (1996) The raw starch binding domain of cyclodextrin glycosyltransferase from *Bacillus circulans* strain 251. *J. Biol. Chem.* **271**, 32777–32784
18. Fersht, A.R., Shi, J.P., Knill-Jones, J., Lowe, D.M., Wilkinson, A.J., Blow, D.M., Brick, P., Carter, P., Waye, M.M., and Winter, G. (1985) Hydrogen bonding and biological specificity analysed by protein engineering. *Nature* **314**, 235–238
19. Street, I.P., Armstrong, C.R., and Withers, S.G. (1985) Hydrogen bonding and specificity. Fluorodeoxy sugars as probes of hydrogen bonding in the glycogen phosphorylase-glucose complex. *Biochemistry* **25**, 6021–6027
20. Xie, H., Bolam, D.N., Nagy, T., Szabo, L., Cooper, A., Simpson, P.J., Lakey, J.H., Williamson, M.P., and Gilbert, H.J. (2001) Role of hydrogen bonding in the interaction between a xylan binding module and xylan. *Biochemistry* **15**, 5700–5707
21. Nagy, T., Simpson, P., Williamson, M.P., Hazlewood, G.P., Gilbert, H.J., and Orosz, L. (1998) All three surface tryptophans in Type IIa cellulose binding domains play a pivotal role in binding both soluble and insoluble ligands. *FEBS Lett.* **429**, 312–316
22. McLean, B.W., Bray, M.R., Boraston, A.B., Gilkes, N.R., Haynes, C.A., and Kilburn, D.G. (2000) Analysis of binding of the family 2a carbohydrate-binding module from *Cellulomonas fimi* xylanase 10A to cellulose: specificity and identification of functionally important amino acid residues. *Protein Eng.* **13**, 801–809
23. Le Gal-Coeffet, M.F., Jacks, A.J., Sorimachi, K., Williamson, M.P., Williamson, G., and Archer, D.B. (1995) Expression in *Aspergillus niger* of the starch-binding domain of glucoamylase. Comparison with the proteolytically produced starch-binding domain. *Eur. J. Biochem.* **233**, 561–567
24. Dalmia, B.K., Schutte, K., and Nikolov, Z.L. (1995) Domain E of *Baccillus macerans* cyclodextrin glucanotransferase: An independent starch-binding domain. *Biotechnol. Bioeng.* **47**, 575–584
25. Iefuji, H., Chino, M., Kato, M., and Iimura, Y. (1996) Raw-starch-digesting and thermostable α-amylase from the yeast *Cryptococcus* sp. S-2: purification, characterization, cloning and sequencing. *Biochem. J.* **318**, 989–996
26. Southall, S.M., Simpson, P.J., Gilbert, H.J., Williamson, G., and Williamson, M.P. (1999) The starch-binding domain from glucoamylase disrupts the structure of starch. *FEBS Lett.* **447**, 58–60
27. Hiromi, K., Nitta, Y., Numata, C., and Ono, S. (1973) Subsite affinities of glucoamylase: examination of the validity of the subsite theory. *Biochim. Biophys. Acta* **302**, 362–375
28. Alkazaz, M., Desseaux, V., Marchis-Mouren, G., Payan, F., Forest, E., and Santimone, M. (1996) The mechanism of *porcine pancreatic* α-amylase. Kinetic evidence for two additional carbohydrate-binding sites. *Eur. J. Biochem.* **241**, 787–796